J Solid State Electrochem (1999) 3: 193–204

ORIGINAL PAPER

Georgios Patermarakis · Konstantinos Moussoutzanis
Nikolaos Nikolopoulos

Investigation of the incorporation of electrolyte anions in porous anodic Al_2O_3 films by employing a suitable probe catalytic reaction

Received: 30 July 1998 / Accepted: 30 September 1998

Abstract A new method has been developed capable of describing the incorporation of electrolyte anions along the pore wall surface and across both the barrier layer and the pore wall oxide after the establishment of the steady state of growth of porous anodic Al_2O_3 where other methods cannot be applied to obtain reliable results. The knowledge of the nature/composition of anodic oxides as regards the incorporation of species like electrolyte anions is of specific importance for both the understanding of the electrochemical mechanism of oxide production and growth and the scientific and technological applications of porous anodic Al_2O_3 films. The method consists of the selection and use of a suitable catalytic probe reaction on porous anodic oxides at thicknesses varying from a value near zero up to the maximum limiting thickness and the treatment of the experimental reaction rate results by a properly developed mathematical formalism. This method was employed in anodic Al_2O_3 films prepared in H_2SO_4 anodizing electrolyte at a constant bath temperature and different current densities using as a probe reaction the decomposition of HCOOH on these oxides, which is almost exclusively a dehydration reaction, at relatively high reaction temperatures, 350 °C and 390 °C, where the effect of other species except SO_4^{2-} incorporated in the oxide on the reaction rate is eliminated. It has been shown that the fraction of the intercrystallite surfaces occupied by SO_4^{2-} follows a parabola-like distribution. It has a significant value at the pore base surface, depending on the current density, then it passes through a maximum along the pore wall surface and across both the barrier layer and the pore walls near the pore bases at positions depending on the current density and then becomes almost zero at the mouths of the pores of the oxide with the maximum limiting thickness and at both the Al_2O_3/Al interface and cell boundaries. The maximum value of the surface coverage is almost independent of the current density and is always near 1, showing an almost complete saturation of intercrystalline surfaces at these positions. The above distribution of surface coverage predicts a qualitatively similar distribution of the SO_4^{2-} bulk concentration across both the barrier layer and pore wall oxide around the pore bases. The method may be improved and developed further either for a more detailed investigation of the above films or to investigate films prepared in other pore-forming electrolytes.

Key words Anodizing · Aluminium · Porous oxide · Electrolyte anions · Incorporation

G. Patermarakis (✉) · K. Moussoutzanis · N. Nikolopoulos
Department of Chemical Engineering,
Section of Materials Science and Engineering,
National Technical University of Athens, Greece
Tel.: +30-33-17723203, Fax: +30-33-17723184

Introduction

Extensive experimental work up to now [1–8] has shown that the nature/composition of the barrier-type anodic Al_2O_3 films formed in different non-pore-forming electrolytes, like phosphates [1–6, 8], chromates [5, 8], oxalates [5], nearly anhydrous maleate solution [7] and other electrolytes like silicate, permanganate, arsenate, selenate, vanadate and sulfate [8], is variable along the cross section of the film. Because the oxide layer is flat it is convenient to use different analytical experimental techniques to examine these films. Such experimental techniques are radiotracer [1], secondary ion mass spectrometry [2], analytical transmission electron microscopy (TEM) of film sections prepared by ultramicrotomy and subsequent electron beam-induced crystallization together with energy dispersive X-ray (EDX) spot analyses [3, 4], auger electron spectroscopy (AES) with ion etching and direct electronoptical examination [5], chemical sectioning combined with impedance measurements [6], Fourier transform infrared (FTIR), AES, scanning electron microscopy (SEM), TEM, STEM/EDX, laser microprobe mass

spectrometry [7], Rutherford backscattering spectroscopy and nuclear reaction analysis [8].

It was shown that two successive layers are generally distinguished besides some few cases of the last group of the above electrolytes, for which uniform layers were observed and electrolyte anions and relevant species were not incorporated at significant amounts. The first layer lying towards the oxide surface is an Al_2O_3 oxide contaminated with electrolyte anions (and probably with other species produced from these anions) and H_2O either as molecular H_2O or OH^- groups and H^+ in the cases of aqueous electrolyte solutions. The second layer towards the oxide/Al interface is a relatively pure oxide in which generally the above species may be detected at much lower or negligible amounts. The ratio of the thickness of these two layers and the profiles of the variations of the concentrations of the above species depend on the conditions of the anodic oxidation and the kind of anodizing electrolyte. The total thickness of the oxide, the separate thicknesses of the two layers, their composition and its variation across them evidently affect significantly different properties, like reactivity, dielectric value, breakdown voltage, etc., and their application such as dielectrics in electrolytic condensers, etc.

Little experimental work compared to that related to the barrier-type oxides has been done for the variation of the composition of the oxide across the barrier layer or the pore wall material of the porous anodic Al_2O_3 films, for the evident reasons that the existence of pores in the porous layer makes these materials inconvenient for the application of the above experimental techniques. Anodic films prepared in phosphoric, oxalic and sulfuric acid pore-forming electrolytes were examined by the experimental techniques of ion beam thinning and TEM [9]. It was suggested that the pore wall material corresponding to each cell of oxide, and as expected the barrier layer of the oxides, also roughly consists of two layers, one lying towards the pore wall and pore base surface being contaminated as previously and the other towards the cell boundaries and the oxide/Al interface being relatively pure Al_2O_3; also the first layer is generally less crystalline than the second one. In a more recent work [10], using the AES experimental technique, the composition of the initially formed flat barrier layer at the very early stages of anodization, and prior to the appearance of the porous layer, as regards the incorporation of the electrolyte anions and related species was investigated for oxides prepared in the above pore-forming electrolytes.

It was postulated that the species due to the anodizing electrolytes incorporated inside the oxide are PO_4^{3-}, $C_2O_4^-$ and SO_4^{2-}, while the elements P, C and S coming from these species follow a bell-like distribution along the cross section of the oxides. Their concentration at the oxide surface is significant and increases appreciably with oxide thickness. Its value becomes a maximum inside the oxide at a distance increasing with oxide thickness and this value becomes highest at an intermediate thickness, at least for the C and S elements. Then, their concentration decreases and becomes almost zero at the oxide/metal interface. Evidently, this suggestion appears to be more realistic considering that there are roughly two distinct layers, a contaminated layer and a relatively pure one inside the barrier layer and pore wall oxide [9].

On the other hand, the distribution of the electrolyte anions across the flat barrier layer oxide may be different from that inside both the hemispherical shell-shaped barrier layer after the complete formation of pores and the pore wall material of each cell near the pore base region. The complete formation of pores is consistent with the establishment of a steady state with respect to the rates of oxide production at the oxide/Al interface and the field assisted dissolution of oxide at pore bases [11], the constant thickness of the barrier layer, the composition of oxide across the barrier layer and the rate of the porous film growth [12]. The existence of the porous layer above the barrier layer and the hemispherical shell-shaped barrier layer prohibit the applicability of the most reliable analytical techniques for the analysis of the barrier layer, while a suitable reliable technique to examine and describe the composition of the pore wall material of one (or of each) cell cannot be conceived.

Knowledge of the composition of the oxide across the barrier layer is of specific importance. Because the pores generally broaden towards the film surface owing to both the chemical dissolution effect of the electrolyte inside the pores during the oxide growth and the mechanism of oxide growth, this composition is extrapolated on the pore wall surface from the pore bases towards the pore mouths. So the variation of oxide composition from the pore base surface up to the oxide/Al interface is extrapolated along the whole length of the pore walls of the oxide with the maximum limiting thickness. In this way the variation of the composition of the oxide across the barrier layer determines the nature/composition and properties of the pore wall surface material. Inversely, the determination of the variation of the oxide composition along the pores can yield the determination of the variation of the oxide composition across the barrier layer. Based on the above-mentioned extrapolation of the nature/composition of the oxide across the barrier layer along the pore wall surface, a new and sensitive method to determine the composition of the oxide along the pores and across the barrier layer of the porous anodic Al_2O_3 films was conceived which, together with a first application of this method, is described in this study.

It is well known that processes very sensitive to the nature/composition of the surface of a solid and the kinds and concentrations of species present on it can generally be suitable reactions heterogeneously catalysed by this surface; even a slight change of the composition of the surface can yield a strong variation of the reaction rate and/or of the selectivity in the cases of multi-way reactions. The new idea appearing in this paper is that the choice of a suitable probe reaction catalysed by the porous anodic oxides and treatment of the relevant re-

sults of the reaction rate and selectivity can yield both the variation of the local composition of the oxide along the pore wall surface and, using a suitable mathematical analysis, this variation across the barrier layer.

The most usually used oxides for scientific and technological applications [13–18], and therefore the most important ones, appear to be the H_2SO_4 films. For chemical alumina [19–22] as well as for H_2SO_4 porous anodic Al_2O_3 [23] there is a suitable probe reaction: the decomposition of HCOOH. Generally, this molecule decomposes in two ways: dehydration ($HCOOH \rightarrow H_2O + CO$) and dehydrogenation ($HCOOH \rightarrow CO_2 + H_2$). Pure chemical alumina exerts almost exclusively a dehydrative action. However, it is well known that the SO_4^{2-} ions in solutions of H_2SO_4 exert also an almost exclusively dehydrative action on HCOOH, producing CO (laboratory method for CO preparation), and the same is expected to be valid for the SO_4^{2-} ions present on the alumina surface. Nevertheless, the activity of these ions must be very different from that of the pure alumina surface.

Consistent with the above, it was indeed shown that the first reaction almost exclusively takes place on the anodic alumina with a selectivity percentage $\cong 100\%$ [23]. In addition, the factors which affect the reaction rate are solely the surface concentration of SO_4^{2-} on the pore walls and the crystallite size, while consistent with the mechanism of the reaction, other species like OH^- and H_2O probably existing on the pore walls do not affect the rate of reaction, at least at the relatively high temperatures, >270 °C, where the reaction rate becomes measurable [23]. For these reasons the decomposition of HCOOH appears to be an excellent probe reaction to study the composition of oxide along the pores and across the barrier layer for films prepared in the H_2SO_4 electrolyte. In the present study, this composition as regards the incorporated SO_4^{2-} ions is examined for first time using the probe reaction. The variations of the fractions of the surfaces of microcrystallites constituting the compact oxide of the barrier layer and of the pore walls [24] occupied by SO_4^{2-} along the pore wall surface and across the barrier layer are described. The variation of the SO_4^{2-} bulk concentration across the barrier layer is also discussed in view of the variation of the above surface fraction across it.

Experimental

Preparation of the porous anodic Al_2O_3 films

The porous anodic Al_2O_3 films were prepared by the anodic oxidation of Al sheets 0.5 mm thick and 99.5% pure. The Al metal composition, the shape and the dimensions of both the Al anode and Pb cathodes employed and the procedure for the treatment of Al specimens prior to the anodization, the washing, neutralization to remove H_2SO_4 remaining inside the pores, washing and drying of the anodized specimens were all outlined in detail previously [12]. Each specimen, 30×50 mm, was divided into 25×5 mm strips parallel to the 30 mm specimen side and kept together by a 50×5 mm strip parallel to the 50 mm upper specimen side (Fig. 1). Each specimen had a tailing end 50×10 mm perpendicular to this strip and originating from the middle of the 50 mm side, which was covered with an insulating varnish, leaving only a small bare part at the edge for electrical connection. In this way the accuracy of the surface area of the Al specimen to be anodized, 33 cm^2, was assured.

The anodization of the Al specimens was performed galvanostatically in a thermostatically controlled and non-stirred bath of H_2SO_4 (15% w/v) at a bath temperature of 30 °C and current densities of 5, 15 and 35 mA cm^{-2}. Different anodization times were used to produce different film thicknesses between a value near zero and the maximum limiting film thickness; the maximum limiting film thickness is established at prolonged anodization as a result of the general broadening of pores towards the film surface [12]. The method for the determination of the film thickness was described in detailed previously [12]. The real surface area of the porous anodic oxides was determined by the Brunauer, Emmett and Teller (BET) method.

After completion of the anodic oxidation, washing, neutralization, washing and drying of the anodized specimens, the tailing ends of the specimens were cut. The strips into which the Al specimen was divided prior to anodization were separated by cutting appropriately the strip, keeping them together at the top of the Al specimen, and ten 30×5 mm strips were thus formed, with a total oxidized geometric surface area of 33 cm^2, which were used in the probe reaction.

Experimental setup and procedure for the probe catalytic reaction

For the probe catalytic reaction, a classical Schwab differential laboratory microreactor was employed [25]. The reactor setup comprised the container of liquid HCOOH, the evaporator, the reactor chamber and the condenser where the unreacted gaseous HCOOH and the product H_2O were condensed. The reactor operated differentially as a continuous flow system. The operation conditions were such that the dilution of the condensed HCOOH by the product H_2O was always negligible, permitting the mixing of the condensates with the HCOOH during each run, while the rate of HCOOH decomposition was not affected. The reaction rate was measured by the flow rate of the product gases at room temperature. The whole setup operated at atmospheric pressure. The composition of the gas mixture and therefore the reaction selectivity value was determined by a gas chromatography analyzer connected in series with the flow meter system.

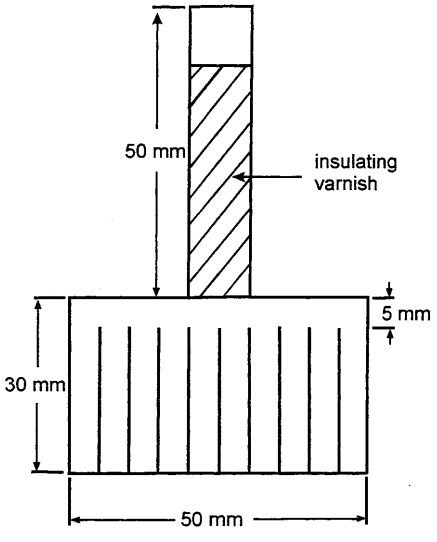

Fig. 1 Schematic representation of the shape and dimensions of the Al specimens which were anodically oxidized

The measurements of the reaction rate were obtained at various temperatures by a dynamic method. The reactor temperature increased linearly with time, initially at a rate of ≅10 °C min^{-1} from room temperature up to a temperature at which the HCOOH decomposition reaction produced a measurable reaction rate, which was always >270 °C. Then the temperature was regulated to increase at a rate of ≅2 °C min^{-1} up to the highest employed temperature of 390 °C. In order to reveal and control both phenomena of catalyst deactivation with operation time and probable hysteresis phenomena between the true average reaction temperature and that measured arising from the finite rate of heat transfer inside the reactor chamber, which were described in detail previously [23], the temperature was regulated to decrease at the same rate to 270 °C; then the above temperature scanning operation was also repeated successively twice up and down over the temperature range of 270–390 °C.

During the above operation a decrease of the initial activity of the oxide relevant to each constant temperature took place and a steady state was finally achieved in which the reaction rate remained constant with time while hysteresis phenomena were not detected. This steady state was generally always established well before the elapse of the time interval necessary to complete the fourth scanning operation from 390 °C to 270 °C and for this reason the results of the fifth scanning operation from 270 °C to 390 °C were taken into consideration. The time interval necessary to complete each experiment was ≅6 h. The measurements at two significantly different temperatures, 350 °C and 390 °C, were taken into consideration. These temperatures were significantly different and sufficiently high such that the decisive factors for the probe reaction at each position on the pore walls were the local surface concentration of SO_4^{2-} and the local size of the microcrystallites, but not the presence of H^+ and OH^- groups which are quickly condensed to H_2O and desorb as the mechanism of the reaction anticipates [23].

The order of reaction in the reaction conditions was determined by the following methodology. Mixtures of HCOOH and H_2O at HCOOH molar fractions of 1.0, 0.95 and 0.9 were used. After the probe catalytic reaction experiment the temperature scanning operations up and down over the temperature range of 270–390 °C were further repeated three times using one molar fraction mixture each time. The latter experimental procedure was employed after each probe catalytic reaction experiment concerning the most and the least active oxides prepared at each current density (see later). The reaction rate values at each temperature obtained in the third to sixth temperature scanning operations up and down over the temperature range of 270–390 °C always essentially coincided, showing that the apparent order of reaction in the experimental conditions is zero for all the anodic Al_2O_3 films employed. As previously shown [23], this means that during the probe catalytic reaction the HCOOH saturates the real active surface of the porous anodic Al_2O_3 films.

Results and discussion

Variation of the film thickness (or of the pore length) and of the pore wall real surface area with the anodic oxidation time and current density for oxides prepared in the H_2SO_4 pore-forming electrolyte. Dependence of the pore wall real surface area on the film thickness.

Structural features of the anodic Al_2O_3 films used

Porous anodic Al_2O_3 films are formed by the anodic oxidation of Al in electrolytes which sparingly dissolve the Al_2O_3 produced, like sulfuric, phosphoric, oxalic acids, etc. [13, 14] (pore-forming electrolytes). Their thickness can reach many tens of micrometres. The structure of porous anodic Al_2O_3 films is characterized as a close packed array of approximately hexagonal columnar cells, each of which contains an elongated, roughly cylindrical, pore extending between the external film surface and the Al_2O_3/Al interface, where it is sealed by a thin, compact barrier-type oxide layer [13, 14, 26–29]. The thickness of the barrier layer that is reduced per unit of the imposed anodization voltage is always <14 Å V^{-1} [13, 14]. This structure is schematically depicted in Fig. 2.

The pore/cell surface concentration (n), of the order of 10^{10} cm^{-2} [12], depends solely on the apparent current density (j) (current/geometric surface area of the Al specimen) and the pore base diameter (D_b) on the temperature around the pore bases during the oxide formation [30]. The real pore shape depends on the conditions of preparation and usually it is that of a cylinder, truncated cone or trumpet [12, 30, 31]. The shape of the pores at the preparation conditions employed is approximately that of a truncated cone [12], as shown in Fig. 3 where the sections of an elongated columnar cell and of the corresponding pore of a film with the maximum limiting thickness h_c (film surface AB) and those of a film with a lower thickness h (film surface CH) are depicted.

The values of the total mean film thickness (h) and the total real surface area (S) of oxide spread over the 33 cm^2 of the oxidized geometric surface area (S_g) of the anodized Al specimens at a constant bath temperature of 30 °C and at the different current densities and anodic oxidation times (t) employed are given in Table 1. The anodization voltage was about 8.7, 12.6 and 16.6 V at $j = 5$, 15 and 35 mA cm^{-2}. Therefore the thickness of the barrier layer is <121.8, 176.4 and 232.4 Å correspondingly, i.e. insignificant in comparison to the thicknesses of the films used. Since the thickness of barrier layer is negligible in comparison to that of the porous layer for relatively thick films, as in the present case, the total mean film thickness is approximately equal to the thickness of the porous layer or the length of the pores.

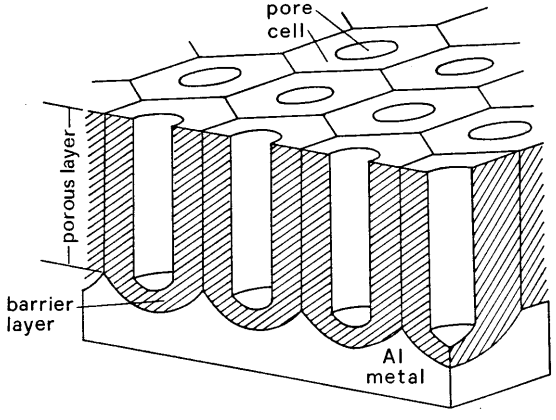

Fig. 2 Schematic representation of the hexagonal columnar cell structure of the porous anodic Al_2O_3 films

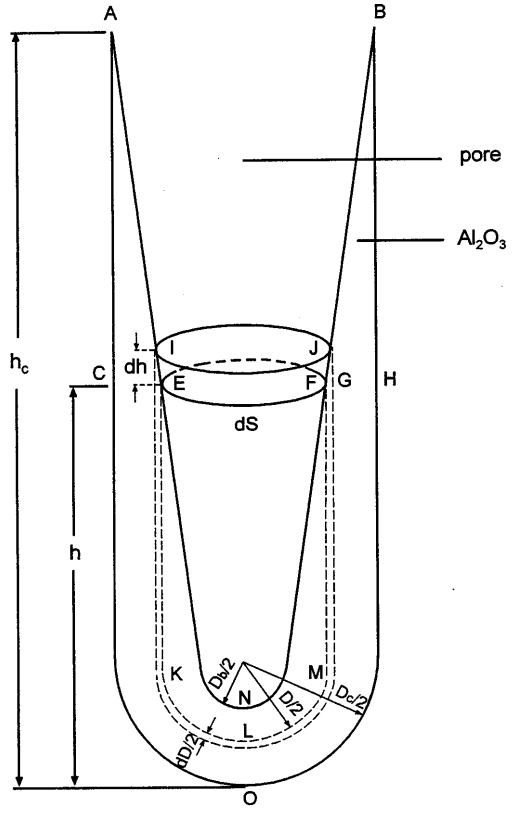

Fig. 3 Schematic representation of a section parallel to the pore axis of an elongated, columnar cell of a film with the maximum limiting thickness

The variation of S/h with h is shown in Fig. 4. The experimental results are fitted well by a linear equation of the form

$$S/h \cong a' + b'h \text{ or } S \cong a'h + b'h^2 \quad (1)$$

By the least squares method the values of a' and b' were found to be $a' = 1.412 \times 10^5$, 0.956×10^5 and 0.789×10^5 and $b' = 3.958 \times 10^9$, 2.034×10^9 and 1.160×10^9 corresponding to $j = 5$, 15 and 35 mA cm^{-2} when h is expressed in meters. Other structural features like cell/pore surface densities and pore base diameters were determined elsewhere [12]. They were $n = 3.69 \times 10^{10}$, 2.93×10^{10} and 2.30×10^{10} cm^{-2} and $D_b = 349$, 336 and 349 Å corresponding to $j = 5$, 15 and 35 mA cm^{-2}. The pore diameter at the mouths of the pores in films with the maximum limiting thickness equals the average cell width, which is determined as the mean value of the lower and higher hexagon cell diameters. It depends solely on n, and is 603, 676 and 763 Å for $j = 5$, 15 and 35 mA cm^{-2}, respectively.

Dependence of the rate of the HCOOH decomposition (dehydration) probe catalytic reaction on the position along the pores of the porous anodic Al_2O_3 films

The analysis of the products of the decomposition of HCOOH on the oxides used by the gas chromatography analysis method showed that the reaction taking place was always an ≅100% dehydration reaction ($HCOOH \rightarrow CO + H_2O$). By the method described previously the order of reaction in the experimental conditions was found to be zero. The values of the rate (r) of the probe reaction on the oxides used at reaction temperatures of 350 °C and 390 °C are given in Table 1.

Table 1 Values of the film thickness (h), the total real surface area (S) of oxide spread over the 33 cm^2 of the oxidized geometric surface area of the anodized specimens at a bath temperature of 30 °C and at different current densities (j) and anodic oxidation times (t). The rate of HCOOH decomposition (dehydration) probe reaction (r) on these oxides is also given at reaction temperatures of 350 °C and 390 °C

j (mA cm^{-2})	t (min)	h (μm)	S (m^2)	$10^7 r$ (350 °C) (mol s^{-1})	$10^6 r$ (390 °C) (mol s^{-1})
5	10	1.5	0.22	2.79	1.13
	15	2.3	0.35	3.33	1.25
	20	3.1	0.47	3.29	1.15
	25	3.9	0.60	3.88	1.25
	30	4.6	0.73	4.45	1.46
	35	5.4	0.87	5.72	2.10
	40	6.2	1.04	9.53	4.15
	60	7.0	1.20	14.69	6.48
	80	7.5	1.24	15.53	8.06
	100	7.5	1.24	13.82	7.05
15	5	2.3	0.23	1.62	0.73
	10	4.6	0.49	2.26	0.81
	10	4.6	0.49	2.77	1.32
	15	7.0	0.76	3.11	1.22
	20	9.3	1.05	3.41	1.25
	20	9.3	1.05	4.22	1.58
	25	11.6	1.38	4.05	1.47
	30	13.9	1.73	5.75	2.34
	35	16.2	2.09	9.56	4.45
	40	17.5	2.27	10.55	5.27
	60	20.0	2.75	23.10	12.29
	80	20.0	2.75	24.19	12.67
	100	20.0	2.75	27.70	14.53
35	5	5.4	0.46	1.54	0.71
	10	10.8	1.00	1.55	0.77
	10	10.8	1.00	3.02	1.30
	15	16.2	1.59	2.71	1.25
	20	21.6	2.21	4.27	2.27
	20	21.6	2.21	3.81	1.72
	25	27.0	2.99	11.05	5.64
	30	32.4	3.66	24.26	12.38
	35	37.9	4.68	55.93	28.81
	50	38.0	4.77	61.18	31.92
	75	38.0	4.77	63.52	31.86
	100	38.0	4.77	54.47	28.55

From the results in Table 1 a sigmoidal variation of r with both h and S is easily verified. The variation of the specific activity (r/S) with S at reaction temperatures of 350 °C and 390 °C is shown in Fig. 5a and b, respectively; a qualitatively similar variation of r/S with h is easily verified. For each j value the r/S value varies strongly with S (or h) and passes through a minimum. It also varies strongly with j for each constant S (or h) value. The value of r/S obtained with the maximum limiting thickness film passes through a minimum at j ≅15 mA cm^{-2}. The r/S versus S variation anticipates a strong heterogeneity of the pore wall surface with a

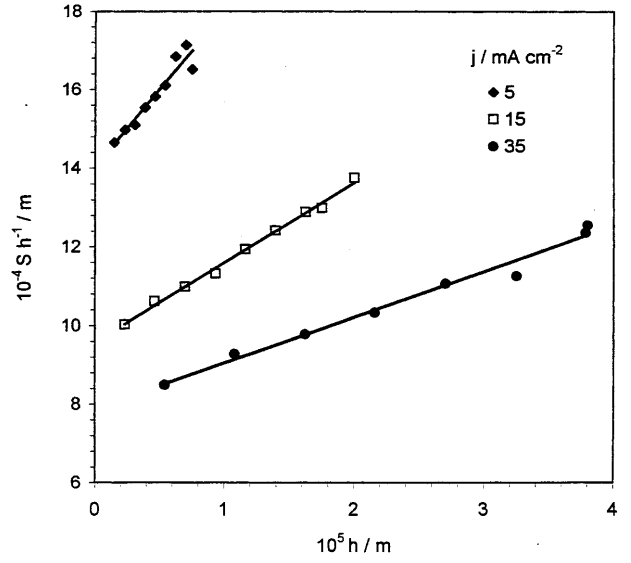

Fig. 4 Variation of the ratio of the total real surface of oxide present over the 33 cm^2 oxidized geometric surface area of the Al specimen to the oxide thickness (Sh^{-1}) with the thickness (h) of oxides prepared at $j = 5$, 15 and 35 mA cm^{-2}

regular and well described pattern according to which the local catalytic activity on the pore wall surface decreases strongly from the pore base towards the pore mouths up to a point on the pore walls specific for each j and then it increases strongly towards the pore mouths.

By the least squares method it was shown that the r/S versus S variation can be described well by a second-order polynomial equation for both the reaction temperatures of 350 °C and 390 °C, i.e.

$$rS^{-1} = a + bS + cS^2, \quad a > 0,\ b < 0,\ c > 0 \tag{2}$$

The values of the a, b and c parameters are given in Table 2. The above equation predicts minima in the rS^{-1} versus S plots for S values satisfying the condition $\mathrm{d}(rS^{-1})/\mathrm{d}S = 0$, i.e. for the $S'_{\min} = -b(2c)^{-1}$ values.

Because the measured catalytic activity rS^{-1} is the integrated one over the whole pore wall surface area S extending between the pore base and the position at a distance h from the pore base, the $S'_{\min}$ and/or the corresponding $h'_{\min}$ value (determined from the $S'_{\min}$ value and Eq. 1) do not define the position on the pore walls where the local activity becomes a minimum. Nevertheless, this position can be found by the following analysis.

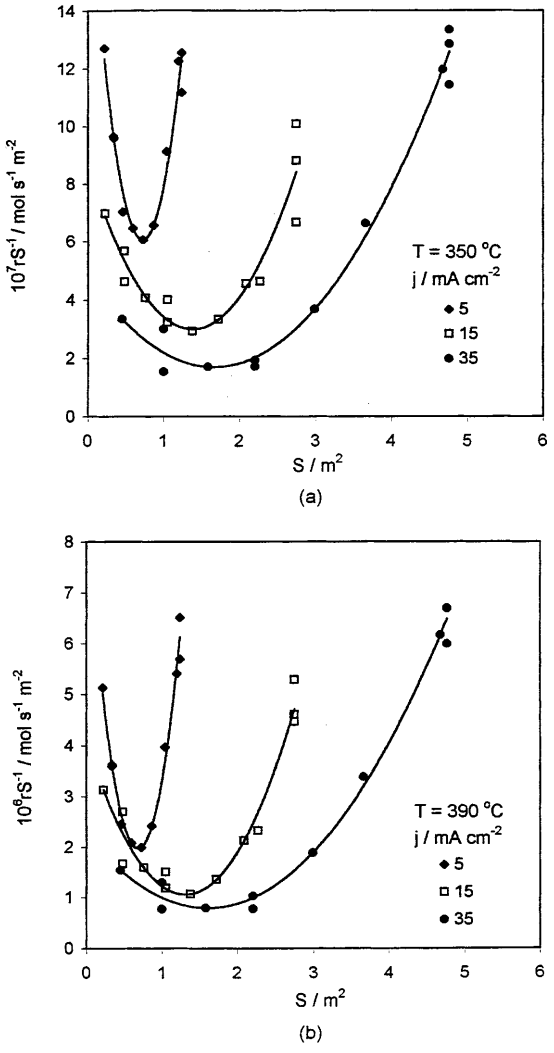

Fig. 5 Variation of the average over the whole real surface specific activity of oxide in the probe reaction (rS^{-1}) with the real surface area (S) at $j = 5$, 15 and 35 mA cm^{-2} and at reaction temperatures of 350 °C (**a**) and 390 °C (**b**)

A ring-shaped differential surface dS on the pore wall surface of a pore (EFJI) is considered as shown in Fig. 3. Its local activity should be equal to $(nS_g)^{-1}(\mathrm{d}r/\mathrm{d}S)$ and for the total number of pores on the whole film surface this activity should be $\mathrm{d}r/\mathrm{d}S$. From Eq. 2 it is inferred that

$$r = aS + bS^2 + cS^3 \tag{3}$$

Table 2 Values of the parameters a, b, c, $S_{\min} = S_{\mathrm{d}r/\mathrm{d}S\,=\,0} = -b(3c)^{-1}$, $h_{\min}$, and $h_{\min}/h_c$ derived from the fitting of the experimental r/S versus S results by a second-order polynomial equation of the form $r/S = a + bS + cS^2$

T (°C)	j (mA cm^{-2})	$10^7 a$ (mol s^{-1} m^{-2})	$10^7 b$ (mol s^{-1} m^{-4})	$10^7 c$ (mol s^{-1} m^{-6})	$S_{\min}$ (m^2)	$h_{\min}$ (μm)	$h_{\min}/h_c$
350	5	18.95	−35.39	24.31	0.49	3.2	0.42
350	15	8.60	−8.08	2.91	0.92	8.2	0.41
350	35	4.85	−3.78	1.13	1.11	12.0	0.32
390	5	85.58	−19.10	138.35	0.46	3.0	0.40
390	15	41.17	−46.60	17.74	0.88	7.8	0.39
390	35	22.62	−18.33	5.70	1.07	11.6	0.31

and

$$dr/dS = a + 2bS + 3cS^2 \quad (4)$$

It is easily derived that the above function also has a minimum at a position S_{min} for which

$$d(dr/dS)/dS = d^2r/dS^2 = 0$$

or

$$2b + 6cS_{min} = 0$$

or

$$S_{min} = -b(3c)^{-1} \quad (5)$$

The S_{min} values thus found are given in Table 2. The corresponding h_{min} values, predicted from the S_{min} values and Eq. 1, and the ratios h_{min}/h_c are also given in Table 2. It is observed that this ratio is almost independent of the reaction temperature. It is also independent of the apparent current density j for $j \leq 15$ mA cm^{-2} but it becomes significantly lower at higher j values.

Formulation of mathematical models describing the dependence of the fraction of the intercrystalline surfaces occupied by the electrolyte anions on the position along the pore wall surface

The mechanism of the porous layer formation after the establishment of the steady state as regards the geometry and nature/composition of the barrier layer [13, 14] predicts that the Al metal is consumed, producing oxide at the Al/oxide interface, and that the oxide dissolves at the pore base by a field-assisted process towards the metal side at equal rates (length/time), so that the thickness of the barrier layer remains constant, leaving behind the porous layer with the characteristic columnar cell structure. Simultaneously, pores are enlarged towards the film surface as a result of the dissolution of the pore wall material by a purely chemical process so that the pores acquire a truncated cone shape in the experimental conditions of the present study [12].

Therefore, the mechanism of the porous layer formation provides that the nature of the oxide at each point on the pore wall surface (i.e. E or F in Fig. 3) will be identical to that of the corresponding position inside the barrier layer oxide or the hemispherical surface (i.e. K or KLM). The nature/composition of the oxide, determined by the crystallite sizes and the concentrations of the species SO_4^{2-}, OH^- and H_2O, across the barrier layer is extrapolated for a thin oxide layer of thickness comparable to crystallite sizes ≤25 Å or ≤40 Å [9, 32], lying in the vicinity of the pore wall surface, and creates a corresponding surface heterogeneity. Because the size of the SO_4^{2-} ions is much larger than that of the other species like Al^{3+} and O^{2-}, they cannot be incorporated in the bulk of the oxide crystallites but they are incorporated almost exclusively in intercrystalline surfaces.

It is noted that the electrolyte anions SO_4^{2-} adsorbed on the pore wall surface are solely attributed to their incorporation inside the barrier layer during the oxide growth. They cannot be attributed to those contained in the anodizing bath solution filling the pores during the oxide growth since this solution, and every species contained in it, is removed by the successive washing, neutralization, washing and drying as previously [12] described. Also, if the SO_4^{2-} ions adsorbed on the pore wall surface were attributed to the above reason, the distribution of the surface concentration of the SO_4^{2-} ions along the pores should be almost uniform along the whole pore length, which is in opposition to the parabola-like sharp distribution which was found in the present study (see later).

Besides the SO_4^{2-} ions, the only species which can exist on the surface after the oxide preparation and the above treatment are the OH^- and/or H_2O ones; their quantity is minimized after drying and becomes negligible or zero at relatively high temperatures like those employed in the test reaction. During heating the SO_4^{2-} anions cannot be removed as SO_3 molecules, since this should take place at temperatures comparable to those where $Al_2(SO_4)_3$ decomposes, i.e. ≥770 °C [33]; the reaction temperatures are much lower than that.

As previously revealed [23], in the conditions of the catalysis experiments the crystallite sizes and the SO_4^{2-} concentration in the intercrystalline surfaces at a position along the pores are the main factors affecting the catalytic behaviour of the oxide at this position. Among them the effect of SO_4^{2-} concentration is much more significant. The average crystallite size at a position across the barrier layer (and along the corresponding hemispherical surface) is affected mainly by the true current density during the oxide formation and the presence of SO_4^{2-} in the intercrystalline surfaces. It increases on decreasing both the true current density during the oxide formation, i.e. along the NO direction in Fig. 3, and the surface concentration of SO_4^{2-} in the intercrystalline surfaces.

On heating during the catalysis experiments, the crystallite sizes and the SO_4^{2-} concentration in the intercrystalline surfaces across the barrier layer may increase to some extent until a permanent state is established (or tends to be established), at which the crystallite sizes inside the whole barrier layer become comparable and the intercrystalline surfaces probably become (or tend to become) saturated by the SO_4^{2-} in the regions of the barrier layer more enriched with SO_4^{2-}. Nevertheless, because the reaction temperatures are much lower than those at which transformation of the microcrystalline anodic Al_2O_3 to γ-Al_2O_3 takes place (≥850 °C [34]), where significant atomic movements inside the crystallites and their boundaries occur, and in addition because the incorporated SO_4^{2-} ions exist mainly in intercrystalline surfaces, extensive digestion of the crystallites and an extensive increase of their size is prohibited. The above remarks are also valid for the pore wall surface oxide.

Although the crystallite sizes and the SO_4^{2-} concentration in intercrystalline surfaces may increase to some

extent, the aforementioned trends across the barrier layer and along the pore wall surface remain the same as those during the probe reaction experiments. Generally, the decrease of both the SO_4^{2-} concentration and the average crystallite size at a position on the surface causes the increase of the catalytic activity of the oxide for the HCOOH dehydration reaction [23].

Because the HCOOH decomposition reaction is almost exclusively a dehydration reaction and the reaction order is zero, as shown previously [23], the mechanism of the reaction embraces: (1) the dissociative adsorption of HCOOH which saturates the surface and yields adsorbed $HCOO^-$ on Lewis acidic sites (Al^{3+}), and H^+ on the O^{2-} sites of the surface (fast step), (2) the decomposition of formate ions (slow step) yielding both CO, which easily desorbs, and adsorbed OH^- groups on the Lewis acidic sites and (3) the condensation of neighbouring OH^- groups (fast step) producing H_2O which desorbs easily.

Let θ be the fraction of the dS ring-shaped surface increment on the pore walls occupied by the SO_4^{2-} ions adsorbed or incorporated at suitable sites such as

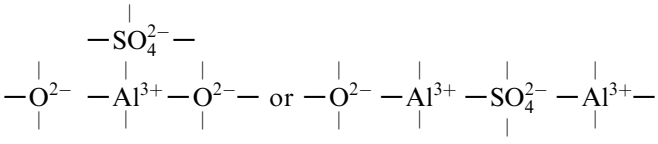

etc., and let $1-\theta$ be the fraction of the surface non-occupied by SO_4^{2-}, i.e.

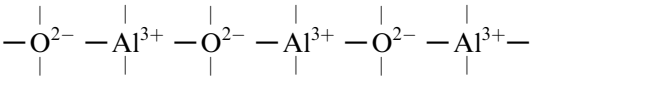

The latter double sites, Al^{3+} and O^{2-}, are the catalytically active sites according to the mechanism of the reaction. Let these sites be characterized by a mean (over the whole non-occupied surface of the crystallites at a position on the pore wall surface) reaction rate constant k referred to the unit of the non-occupied active surface area. The former sites may also have some dehydrative catalytic effect on HCOOH as previously noted. Nevertheless, consistent with earlier experimental results [23] and the experimental results of this study, the dehydrative catalytic efficiency of these sites must be much lower than that of the sites non-occupied by SO_4^{2-}. These less active sites are characterized by a mean (over the whole occupied surface at a position on the pore wall surface) reaction rate constant k' referred to the unit of the surface area occupied by SO_4^{2-}. It is evident that $k \gg k'$. Then, taking into consideration Eq. 4, the local specific activity at a position on the pore walls must be given from

$$\mathrm{d}r/\mathrm{d}S = a + 2bS + 3cS^2 = k(1-\theta) + k'\theta \tag{6}$$

or

$$\theta = [k - (a + 2b + 3cS^2)](k - k')^{-1} \tag{7}$$

It is accepted that the surface concentration of SO_4^{2-} in the intercrystalline surfaces at the Al/oxide interface tends to zero, i.e. $\theta \to 0$. This is well justified from the results of both the electrochemical kinetics and the mechanism of oxide growth [11] and the investigation of the electrolyte anion incorporation in the oxide [10]. Then, the oxide lying near the Al/oxide interface and at the cell boundaries, which is almost free of the presence of SO_4^{2-}, or the oxide surface around the mouths of the pores of a film with the maximum limiting thickness and the maximum possible real surface $S_{\max}$, is characterized by a reaction rate constant k_c which is given from

$$(\mathrm{d}r/\mathrm{d}S)_{S=S_{\max}} = a + 2bS_{\max} + 3cS_{\max}^2 \cong k_c \tag{8}$$

In the oxides heated during the catalysis experiments the average crystallite size at a position inside the barrier layer (σ) also increases with a decrease of both the corresponding true current density during the oxide growth and the surface concentration of SO_4^{2-} in the intercrystalline surfaces. Let σ_b be the average crystallite size at the pore base surface position and σ_c at the Al/oxide interface or at the cell boundaries. The true current density j_t inside the barrier layer is the ratio of the apparent current density j to the hemispherical surface area through which the ionic charge passes during the oxide formation, i.e.

$$j_t = j(2^{-1}\pi n D^2)^{-1} \tag{9}$$

where D is the variable diameter of the hemispherical surface across the barrier layer. This diameter is D_b at pore base and D_c at the Al/oxide interface. It is accepted that the average crystallite size at a position increases linearly with $j_{t,b} - j_t$, where $j_{t,b}$ is the true current density at pore bases, and decreases linearly with θ, i.e.

$$\begin{aligned}\sigma &= \sigma_b + f(j_{t,b} - j_t) - g\theta \\ &= \sigma_b + fj(2^{-1}\pi n)^{-1}(D_b^{-2} - D^{-2}) - g\theta\end{aligned} \tag{10}$$

where f and g are constants. This linear equation is expected to be satisfied better in the cases where j_t and θ do not vary strongly across the whole barrier layer. Considering the Al/oxide interface position, because $nD_c^2 = 4/3$ [11] and $\theta \to 0$, Eq. 10 becomes

$$\begin{aligned}\sigma_c &= \sigma_b + fj(2^{-1}\pi n)^{-1}(D_b^{-2} - D_c^{-2}) \\ &= \sigma_b + j(2^{-1}\pi n D_b^2)^{-1} - fj(2.0944)^{-1}\end{aligned} \tag{11}$$

From the truncated cone-shaped pores it is easily inferred that the D value can be expressed as

$$D = hh_c^{-1}(D_c - D_b) + D_b \tag{12}$$

Using Eqs. 11 and 12, Eq. 10 becomes

$$\begin{aligned}\sigma &= \sigma_c - fj(2^{-1}\pi n)^{-1}(D^{-2} - D_c^{-2}) - g\theta \\ &= \sigma_c - fj(2^{-1}\pi n)^{-1}\{[[hh_c^{-1}(D_c - D_b) + D_b]^{-2} - D_c^{-2}] - g\theta\}\end{aligned} \tag{13}$$

which also gives the average crystallite size at a position on the pore wall surface at a distance h from the pore base.

It is accepted that within a relatively narrow range of crystallite size values the catalytic activity relevant to the free sites (non-occupied by SO_4^{2-}) decreases linearly with the crystallite size, i.e.

$$k = v - w\sigma \tag{14}$$

where v and w are constants. This equation is expected to be satisfied better when the crystallite size varies slightly across the barrier layer. Considering the Al/oxide interface region, or the mouths of the pores of a film with thickness h_c, and Eq. 8, Eq. 14 becomes

$$k_c = v - w\sigma_c = a + 2bS_{max} + 3cS_{max}^2 \tag{15}$$

Then, the local catalytic activity dr/dS becomes

$$\begin{aligned} dr/dS &= a + 2bS + 3cS^2 \\ &= \{v - w\{\sigma_c - fj(2^{-1}\pi n)^{-1} \\ &\quad \times \{[[hh_c^{-1}(D_c - D_b) + D_b]^{-2} - D_c^{-2}] - g\theta\}\}\} \\ &\quad \times (1 - \theta) + k'\theta \end{aligned} \tag{16}$$

and from Eq. 15, Eq. 16 becomes

$$\begin{aligned} &a + 2bS + 3cS^2 \\ &\quad = \{a + 2bS_{max} + 3cS_{max}^2 + \{wfj(2^{-1}\pi n)^{-1} \\ &\qquad \times \{[[hh_c^{-1}(D_c - D_b) + D_b]^{-2} - D_c^{-2}] - g\theta\}\}\} \\ &\qquad \times (1 - \theta) + k'\theta \end{aligned} \tag{17}$$

The latter equation involves the variable θ and the unknown constants f, g, w and k'. Its solution demands knowledge of the values of the above constants, the experimental determination of which needs further investigation, is probably very difficult and is outside the scope of this study.

Simplification of Eq. 17 to an applicable form.
Determination of the fraction of intercrystalline surfaces occupied by SO_4^{2-} along the pore wall surface and across the barrier layer.
Interpretation of the results

Since the local surface concentration of SO_4^{2-} exerts a much stronger effect on the local surface activity than that of the local average crystallite size [23], it can be considered that, to a good approximation, the local average crystallite size on the pore wall surface does not vary considerably and remains almost constant along the pore walls. This is expected to be satisfied better at low film thicknesses. In cases of high thicknesses, like the maximum limiting ones, it is better satisfied for a thinner barrier layer and therefore for lower maximum limiting film thicknesses which are obtained at low j values of oxide preparation, as in the present case. The above hypothesis is strengthened also by the fact that when the oxides are heated at relatively high temperatures, as in the present case during the probe reaction experiments, the crystallite sizes must increase to some extent and become comparable over the whole bulk of the barrier layer and the pore wall oxide, although the trend for their variations across the barrier layer and along the pore wall surface still remains the same as before the probe reaction experiments.

The constancy of the crystallite sizes predicts that $f \cong 0$ and $g \cong 0$ and Eq. 17 becomes

$$a + 2bS + 3cS^2 \cong (a + 2bS_{max} + 3cS_{max}^2)(1 - \theta) + k'\theta \tag{18}$$

Because $k' \ll k$ the term $k'\theta$ can be ignored and the above equation is finally transformed into

$$\theta \cong 1 - (a + 2bS + 3cS^2)(a + 2bS_{max} + 3cS_{max}^2)^{-1} \tag{19}$$

Research into the above equation shows that $d^2\theta/dS^2 < 0$ and therefore it has a maximum (θ_{max}) at a position for which $d\theta/dS = 0$ or at $S = -b(3c)^{-1}$, i.e. exactly at the position S_{min} where the minimum in the local activity, dr/dS, is observed. The variation of θ with S ($0 \le S \le S_{max}$) at various j values is given in Fig. 6a and b for reaction temperatures of 350 °C and 390 °C, respectively. For $S \to 0$ the θ value is always considerable and increases with j. The θ_{max} value is high and always tends to 1. When $S \to S_{max}$, evidently $\theta \to 0$. It is observed that the θ value generally varies only slightly with the reaction temperature and, as expected, it can be considered independent of the reaction temperature.

The variation of the portion of the intercrystalline surfaces occupied by the electrolyte anions across the barrier layer, or across the pore wall oxide of each cell around the pore base region, with thickness $(D_c - D_b)/2$, can be described by the following. A hemispherical surface inside the barrier layer at a distance $(D - D_b)/2$ from the pore base surface is considered. The hemispherical shell defined from the surfaces with diameters D and $D + dD$ will have a thickness $dD/2$, which is considered to be comparable to the average crystallite size. The nature/composition of the oxide in this shell will be identical to that of the oxide contained in the volume on the pore walls defined from the triangle JFG by revolution. Because the inclination of the pore wall relative to the pore axis is very small, tending to zero, then $dh \gg dD/2$ and along the length $JF = [(dh)^2 + (dD/2)^2]^{1/2} \cong dh$ there must be arranged a large number of crystallites. The average θ value relevant to the surface of all the crystallites corresponding to the dS surface will then be almost identical to the θ value corresponding to all crystallite surfaces inside the aforementioned shell. In this way the average θ value at a position inside the barrier layer is justified to be almost identical to that at the corresponding position on the pore walls.

Taking into consideration the truncated cone pore geometry and that the thickness of the barrier layer is negligible in comparison to h, it is easily derived that the ratio of the distance of the above shell from the pore base surface to the thickness of barrier layer (relative depth, r.d.), will be $\text{r.d.} = [2^{-1}(D - D_b)]/[2^{-1}(D_c - D_b)] = h/h_c$. Then, the insertion of Eq. 1, $S = a'h + b'h^2 = a'h_c(h/$

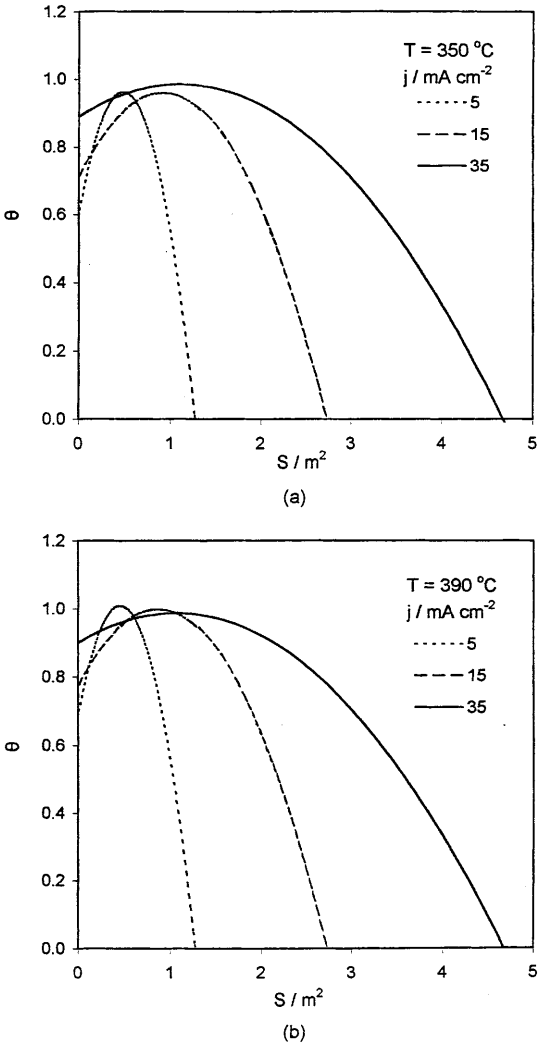

Fig. 6 Variation of the local fraction of the intercrystalline surfaces at a position on the pore wall surface occupied by SO_4^{2-} (θ) with the pore wall real surface (S) of oxide at $j = 5$, 15 and 35 mA cm^{-2} and at reaction temperatures of 350 °C (**a**) and 390 °C (**b**)

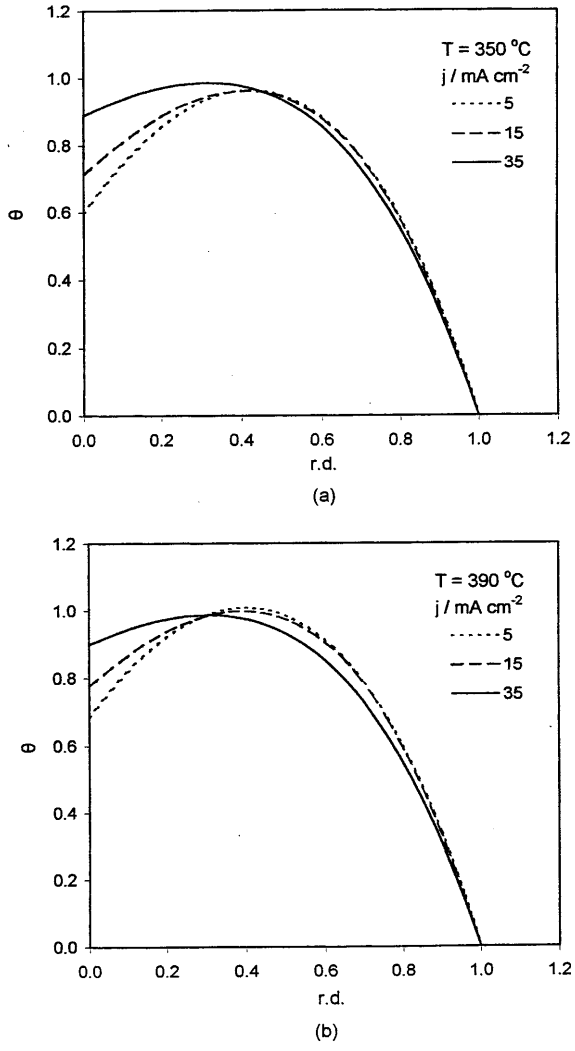

Fig. 7 Variation of the local fraction of the intercrystalline surfaces at a position inside the barrier layer occupied by SO_4^{2-} (θ) with the relative depth (r.d.) of the position inside the barrier layer at $j = 5$, 15 and 35 mA cm^{-2} and reaction temperatures of 350 °C (**a**) and 390 °C (**b**)

$h_c) + b'h^2_c(h/h_c)^2$, into Eq. 19 yields $\theta = \theta(h/h_c)$ or $\theta = \theta$(r.d.). The plots of θ versus r.d. are shown in Fig. 7. These are qualitatively similar to those of Fig. 6 and similar observations are also made. From the values of the thickness of the barrier layer, $(D_c - D_b)/2 = 127$, 170 and 207 Å at $j = 5$, 15 and 35 mA cm^{-2}, respectively, and the r.d. values where the θ_{max} values appear, it is concluded that the θ_{max} positions are buried at a distance of 52, 68 and 66 Å, respectively, from the pore base surface inside the barrier layer.

Because, as noted above, the crystallite sizes do not vary greatly across the barrier layer, the variation of θ across it also represents qualitatively the variation of the bulk concentration of SO_4^{2-} across the barrier layer. Hence the bulk concentration of SO_4^{2-} inside the barrier layer follows a parabola-like distribution qualitatively consistent with previous results relevant to the flat barrier layer prior to the appearance and complete formation of pores [10] where a bell-like distrubition was revealed. The bulk concentration of the SO_4^{2-} ions can be estimated from the θ values, the size of the crystallites and therefore their surface area and the average surface occupied by each SO_4^{2-} ion or the size of this ion. Nevertheless, this is outside the scope of this study. Generally, in each case, considering more or less uniform crystallite sizes across the barrier layer, which is justified in the present case since the oxides were heated at relatively high temperatures for a long enough time, then the variation of θ across both the barrier layer and the pore walls of each cell near the pore base position must be qualitatively similar to the variation of the relevant bulk concentration of the SO_4^{2-} ions.

It is obvious that the above analysis and the geometrical characteristics of the pores can be used to describe the distribution of the θ values across the pore wall oxide at each position on the pore walls. The above-

described profile of θ or of the SO_4^{2-} bulk concentration across the barrier layer is expected to be of specific importance and usefulness for understanding and describing future studies on the electrochemical mechanism of oxide production and growth and its characteristics like ionic migration, transport numbers, etc., much of which is still unknown.

The bell-like distribution of the electrolyte anions across the barrier layer at the very early stages of anodization and prior to the appearance of the porous layer [10] was explained by a reasonable theory, described by suitable equations, involving a field-enhanced ion migration mechanism. During the oxide growth the kinetics of the electrolyte anion flux predicts that the anion concentration is a maximum at the oxide/electrolyte interface and decreases with a decreasing rate towards the oxide/metal interface as a result of the field-enhanced anion migration. The high strength field, the space charge established inside the barrier layer oxide during anodization and the subsequent necessary relaxation phenomena inside the oxide bulk, taking place after the interruption of the anodic oxidation process and during the ageing of the oxide at a constant temperature, yield ionic flux kinetics which finally produce a distribution of the electrolyte anions across the barrier layer qualitatively similar to that determined experimentally [10].

In that analysis and the relevant equations which were employed uniform nature/composition, lattice parameter, activation energy for the ion diffusion/migration, etc., across the oxide layer were considered. Also, a hopping/diffusion mechanism for the ion migration through vacant lattice sites was evidently adopted, denoting that the easy, effective migration paths traverse the bulk of the microcrystallites constituting the oxide. Nevertheless, it is well known that the nature/composition, the crystallite sizes and therefore the intercrystalline surface area per unit of oxide mass or volume, etc., are variable across the barrier layer [9, 10].

Also, because the size of the electrolyte anions is much larger than that of O^{2-}, the electrolyte anions cannot be embodied easily in the bulk of the microcrystallites and therefore they are located rather around the microcrystalline surfaces and most probably the effective paths for the migration of the anions are the intercrystalline surfaces or spaces. Hence, although this theory seems to be correct as regards its origin, it must be an oversimplified one, roughly approximating both the real situation for the kinetics and mechanism of charge transport across the barrier layer and the observed anion distribution across it.

After the establishment of the hemispherical shell-shaped barrier layer, as in the present case, the same theory must be considered valid as a qualitatively similar distribution of the SO_4^{2-} anions across the barrier layer was found. Nevertheless, in the present case a much stronger heterogeneity across the barrier layer as regards the nature/composition of the oxide, the crystallite sizes, the intercrystalline surface area, etc., in comparison to those in the case of the flat barrier layer is established, owing mainly to the variation of the true current density across the barrier layer during the oxide growth; this makes the case even more complex and therefore the above-mentioned theory [10] must be considered even less accurately applicable. In view of the strong variation of the oxide nature/composition, etc., across the barrier layer, the case that the distribution derived in this study, or a qualitatively similar one, is also established during the anodic oxidation process cannot be excluded.

The existence of a maximum θ value always tending to 1, showing an almost complete saturation of the intercrystalline surfaces at the relevant positions inside the barrier layer during the oxide growth, constitutes an indication for the probable validity of the latter suggestion. In this case the mechanism and kinetics of the ionic migrations and charge transport across the barrier layer are expected to be extremely complex. It is apparent that for the elucidation of all these phenomena and the formulation of a reliable theory explaining satisfactorily the derived distribution of anions across the barrier layer, further detailed investigation is necessary.

Conclusions

From the results of the present study the following concluding remarks can be drawn.

1. A new method has been developed capable of describing the fraction of the intercrystalline surfaces occupied by the electrolyte anions along the pores and across both the barrier layer and the pore wall oxide near the pore bases of porous anodic oxide films. Also, the bulk concentration of the electrolyte anions can be described, at least qualitatively. The new method consists of both the use of a suitable probe catalytic reaction over the porous anodic Al_2O_3 films at relatively high temperatures, to avoid involvement of the species OH^-, H^+ and H_2O which are embodied in the oxide at low temperatures, and a suitable mathematical treatment of the experimental results by properly formulated equations.

2. For anodic oxide films prepared in the H_2SO_4 electrolyte, the most suitable probe reaction was judged to be the catalytic decomposition of HCOOH, which is almost exclusively, $\cong$100%, a dehydration reaction of zero order on these anodic aluminas. This probe reaction was employed on anodic oxide films prepared at a constant bath temperature, different current densities and different anodic oxidation times sufficient to produce films with thicknesses varying from a low value near zero and the maximum limiting thickness obtained at each current density. A general mathematical formalism was developed. The resulting equations were complex and a suitable simplification was made on the basis of some reasonable admissions. The mathematical treatment of the reaction rate results obtained at 350 °C and 390 °C showed that the fraction of intercrystalline surfaces occupied by SO_4^{2-} at the pore base surface is

$\cong 0.65$, 0.75 and 0.90 for $j = 5$, 15 and 35 mA cm^{-2}, respectively. Then it passes through a maximum at a position along the pores corresponding to $\cong 0.41h_c$, $0.40h_c$ and $0.32h_c$, respectively, for the above current densities. Then it decreases up to the pore mouths region, where it becomes $\cong 0$. A qualitatively similar distribution of θ with the depth inside the barrier layer is predicted from the mathematical analysis. The maximum is also met at a relative depth inside the barrier layer $\cong 0.41$, 0.40 and 0.32, respectively, at the above current densities. The θ values become $\cong 0$ near the Al/Al_2O_3 interface. This distribution is also valid across the pore wall material near the pore bases. It is worth noting that the θ_{max} value always tends to 1, showing an almost complete saturation of intercrystalline surfaces at the relevant positions, at least for the oxides heated during the probe reaction experiments. The above distribution of θ across the barrier layer must be qualitatively similar to the distribution of the bulk concentration of SO_4^{2-} across it.

3. The method can be improved by the experimental determination of some constants involved in the detailed, complex equations in order to achieve both a higher accuracy of the determination of θ and the determination of the bulk concentration of SO_4^{2-} across the barrier layer and pore wall oxide.

4. Other suitable probe reactions may also be found and employed in anodic oxides prepared in sulfuric acid, as well as in other pore-forming electrolytes like phosphoric and oxalic acid, to investigate the incorporation of the electrolyte anions and other species inside the barrier layer and pore wall material.

5. The method is suitable to investigate porous anodic oxides after the complete formation of pores and the establishment of a steady state as regards the production of oxide at the Al/Al_2O_3 interface, the field assisted dissolution of oxide at pore bases [11] and the growth of the porous layer where other suitable and reliable methods cannot be conceived. The application of other reliable methods like the sputtering and XPS or AES, etc., techniques in the examination of porous anodic Al_2O_3 films can yield only the variation of an average local concentration of the electrolyte anions referred to the total local volume (pore void volume + the volume of compact pore wall oxide) across the porous anodic Al_2O_3 film; the knowledge of such a distribution cannot give as much information as that obtained by the present method. These methods are suitable only for the examination of flat compact oxide layers. The further development of the method presented in this study may yield an excellent tool for the investigation of the nature/composition of oxide across both the barrier layer and pore walls after the establishment of the above-mentioned steady state.

References

1. Randall JJ, Bernard WJ (1975) Electrochim Acta 20: 653
2. Abd Rabbo MF, Richardson JA, Wood GC (1976) Corros Sci 16: 689
3. Thompson GE, Wood GC, Shimizu K (1981) Electrochim Acta 26: 951
4. Shimizu K, Thompson GE, Wood GC (1981) Thin Solid Films 77: 313
5. Xu Y, Thompson GE, Wood GC, Bethune B (1987) Corros Sci 27: 83
6. Takahashi H, Fujimoto K, Nagayama M (1988) J Electrochem Soc 135: 1349
7. Ue M, Asahina H, Mori S (1995) J Electrochem Soc 142: 7
8. Wood GC, Skeldon P, Thompson GE, Shimizu K (1996) J Electochem Soc 143: 74
9. Thompson GE, Furneaux RC, Wood GC (1978) Corros Sci 18: 481
10. Parkhutic VP (1986) Corros Sci 26: 295
11. Patermarakis G, Moussoutzanis K (1995) Electrochim Acta 40: 699
12. Patermarakis G, Lenas P, Karavassilis Ch, Papayiannis G (1991) Elecrochim Acta 36: 709
13. Young L (1961) Anodic oxide films. Academic Press, London
14. Diggle J, Downie T, Goulding C (1969) Chem Rev 69: 365
15. Smith AW (1973) J Electrochem Soc 120: 1068
16. Kawai S, Ishiguro I (1976) J Electrochem Soc 123: 1047
17. Cocke DL, Johnson ED, Merrill RP (1984) Catal Rev Sci Eng 26: 163
18. Skoulikidis T, Patermarakis G (1989) Aluminium 65: 185
19. Krylov O (1970) Catalysis by nonmetals. Academic Press, New York
20. Noto Y, Fukuda K, Onishi T, Tamaru K (1967) Trans Faraday Soc 63: 2300
21. Fukuda K, Noto Y, Onishi T, Tamaru K (1967) Trans Faraday Soc 63: 3072
22. Tamaru K (1978) Dynamic heterogeneous catalysis. Academic Press, London
23. Patermarakis G, Pavlidou C (1994) J Catal 147: 140
24. Patermarakis G, Kerassovitou K (1992) Electrochim Acta 37: 125
25. Anderson RB (ed), Dawson PT (1968) Experimental methods in catalytic research, vol 1. Academic Press, London
26. Keller F, Hunter MS, Robinson DL (1953) J Electrochem Soc 100: 141
27. Wood GC, O'Sullivan JP, Vaszko B (1968) J Electrochem Soc 115: 618
28. Furneaux RC, Thompson GE, Wood GC (1978) Corros Sci 18: 853
29. Xu Y, Thompson GE, Wood GC (1982) Electrochim Acta 27: 1623
30. Patermarakis G, Moussoutzanis K (1995) J Electrochem Soc 142: 737
31. Patermarakis G, Karayianni HS (1995) Electrochim Acta 40: 2647
32. Baker B, Pearson R (1972) J Electrochem Soc 119: 160
33. Weast RC (ed) (1980) Handbook of chemistry and physics, 60th edn. CRC Press, Boca Raton, p. B-52
34. Ruckenstein E, Chu YF (1979) J Catal 52: 109